Published in final edited form as:
Arterioscler Thromb Vasc Biol. 2012 March ; 32(3): . doi:10.1161/ATVBAHA.111.242594.

Inhibition of bone morphogenetic protein signaling reduces vascular calcification and atherosclerosis

Matthias Derwall, M.D., **Rajeev Malhotra, M.D.**, **Carol S Lai, M.S.**, **Yuko Beppu, M.S.**, **Elena Aikawa, M.D., Ph.D.**, **Jasbir S. Seehra, Ph.D.**, **Warren M Zapol, M.D.**, **Kenneth D. Bloch, M.D.***, and **Paul B. Yu, M.D., Ph.D***

Anesthesia Center for Critical Care Research of the Department of Anesthesia, Critical Care, and Pain Medicine (M.D., Y.B., W.M.Z., K.D.B.), the Cardiovascular Research Center and Cardiology Division of the Department of Medicine (R.M., C.S.L., K.D.B., P.B.Y.), the Center for Molecular Imaging Research (E.A.) at the Massachusetts General Hospital and Harvard Medical School, Boston, MA; Acceleron Pharma, Inc (J.S.S.), Cambridge, MA.

Abstract

Objective—The expression of bone morphogenetic proteins (BMPs) is enhanced in human atherosclerotic and calcific vascular lesions. While genetic gain- and loss-of-function experiments in mice have supported a causal role of BMP signaling in atherosclerosis and vascular calcification, it remains uncertain whether BMP signaling might be targeted pharmacologically to ameliorate both of these processes.

Methods and Results—We tested the impact of pharmacologic BMP inhibition upon atherosclerosis and calcification in low density lipoprotein receptor-deficient ($LDLR^{-/-}$) mice. $LDLR^{-/-}$ mice fed a high-fat diet developed abundant vascular calcification within twenty weeks. Prolonged treatment of $LDLR^{-/-}$ mice with the small molecule BMP inhibitor LDN-193189 was well-tolerated and potently inhibited development of atheroma, as well as associated vascular inflammation, osteogenic activity, and calcification. Administration of recombinant BMP antagonist ALK3-Fc replicated the anti-atherosclerotic and anti-inflammatory effects of LDN-193189. Treatment of human aortic endothelial cells with LDN-193189 or ALK3-Fc abrogated the production of reactive oxygen species (ROS) induced by oxidized LDL, a known early event in atherogenesis. Unexpectedly, treatment of mice with LDN-193189 lowered LDL serum cholesterol by 35% and markedly decreased hepatosteatosis without inhibiting HMG-CoA reductase activity. Treatment with BMP2 increased, whereas LDN-193189 or ALK3-Fc inhibited apolipoprotein B100 secretion in HepG2 cells, suggesting that BMP signaling contributes to the regulation of cholesterol biosynthesis.

Conclusions—These results definitively implicate BMP signaling in atherosclerosis and calcification, while uncovering a previously unidentified role for BMP signaling in LDL

Address correspondence to: Matthias Derwall, M.D. Uniklinik Aachen RWTH Aachen University Department of Anesthesia Pauwelsstr. 30 52074 Aachen, Germany Phone: +49 (241) 80 80259 Fax: +49 (241) 80 82406 mderwall@ukaachen.de Paul B. Yu, M.D., Ph.D. Cardiovascular Division Brigham and Women's Hospital 75 Francis Street, Boston, MA 02115 Phone: 857-307-0395 Fax: 857-307-0394 pbyu@partners.org.

*K.D.B. and P.B.Y. contributed equally. M.D. and P.B.Y. current addresses noted below.

Disclosures Massachusetts General Hospital and Partners Healthcare Inc. have applied for patents related to small molecule inhibitors of BMP type I receptors and the application of ALK3-Fc to treat atherosclerosis and vascular calcification, and MD, RM, KDB, and PBY may be entitled to royalties. Jasbir S. Seehra is a former employee of Acceleron Pharma, Inc, the manufacturer of ALK3-Fc.

cholesterol metabolism. BMP inhibition may be helpful in the treatment of atherosclerosis and associated vascular calcification.

Keywords

atherosclerosis; inflammation; lipoproteins; hypercholesterolemia

Introduction

BMP ligands provide critical signals for determining cell fate and embryonic patterning in development, and contribute to the postnatal remodeling of diverse tissues[1]. More than 20 known BMP ligands, which form a subset of the TGF-β family, are recognized by heteromeric complexes of BMP type I and type II serine-threonine kinase receptors on the membrane surface[2]. Ligand binding induces constitutively-active BMP type II receptors to transphosphorylate BMP type I receptors, which in turn phosphorylate the intracellular BMP effector proteins, SMADs 1, 5, and 8 (SMAD1/5/8). “Canonical” signaling via the activation of SMAD1/5/8 and its associated transcriptional co-regulators appear to mediate the principal effects of BMPs, while activation of additional pathways including mitogen-activated protein kinases may further refine cellular effects[3]. BMP signaling is also modulated by extracellular ligand antagonists, such as noggin, and by membrane-associated BMP co-receptors including the repulsive guidance molecules and endoglin[4, 5].

Vascular calcific lesions associated with atherosclerosis, diabetes and chronic kidney disease are known to be enriched in BMP ligands, a host of bone-specific matrix regulatory proteins, and cells with the phenotypic profile of osteoblasts and chondroblasts, whose differentiation is known to be coordinated by BMPs[6-11]. The concept that BMPs regulate vascular calcification is supported by the finding that smooth muscle-targeted overexpression of BMP2 accelerates vascular calcification in atherogenic (apoE$^{-/-}$) mice[12]. Similarly, arterial calcification is observed in mice lacking matrix Gla Protein (MGP), a vitamin K-dependent calcium-binding extracellular matrix protein that inhibits osteogenic differentiation, and which is proposed to function as an endogenous BMP inhibitor[13-15]. In fact, MGP overexpression in apoE$^{-/-}$ mice reduces vascular calcification, as well as antecedent vascular inflammation and atherosclerosis[16], suggesting a role for BMP signaling in early vascular injury as well as calcification. However, MGP-deficient apoE$^{-/-}$ mice are also protected from atherosclerosis, despite developing extensive vascular calcification[16]. Moreover, atherosclerosis is not accelerated in apoE$^{-/-}$ mice overexpressing BMP2 in smooth muscle[12]. While these studies support a causal role of BMP signaling in vascular calcification, there remains some uncertainty about the precise contribution of BMP signaling in atherosclerosis, as well as the causal or mechanistic linkage of atherosclerosis and vascular calcification.

To further delineate the role of BMP signaling in atherosclerosis and vascular calcification, while avoiding the confounding developmental effects of gene disruption or overexpression, we studied the effects of inhibiting BMP signaling postnatally in LDLR$^{-/-}$ mice[17, 18], using a small molecule inhibitor of BMP type I receptor kinases, LDN-193189[19]. We found that pharmacologic blockade of BMP signaling with LDN-193189 is well-tolerated in adult mice, even for prolonged periods of time, as measured by a variety of gross, hematologic, and bone metabolic parameters. Whereas hyperlipidemic vascular injury led to the activation of SMAD1/5/8 in vascular cells and lesions, BMP inhibition using LDN-193189 effectively attenuated the activation of SMAD1/5/8 in these tissues, as well as subsequent inflammation, atherosclerosis, and vascular calcification. BMP signaling inhibition with LDN-193189 inhibited oxidative stress associated with hyperlipidemia and also exerted potent effects upon lipoprotein biosynthesis, reducing serum levels of total cholesterol and

low density lipoprotein (LDL). Importantly, inhibition of BMP ligand activity using a recombinant BMP type I receptor extracellular domain fusion protein, ALK3-Fc[20], also attenuated SMAD1/5/8 activation, inflammation and atherosclerosis *in vivo*. While LDN-193189 and ALK3-Fc both inhibited the synthesis of Apolipoprotein B100 (ApoB) by HepG2 cells in vitro, ALK3-Fc did not reduce serum LDL in hyperlipidemic mice, despite potently inhibiting atherosclerosis. These results obtained using two distinct pharmacologic strategies demonstrate an unequivocal role of BMP signaling in atherosclerosis and vascular calcification that is independent of modifying serum lipids, while highlighting an additional and previously unknown role of BMP signaling in lipoprotein homeostasis. Taken together, these data suggest that treatments targeting this pathway may be useful for modifying atherosclerotic and vascular calcific disease.

Methods

Chemicals and reagents

LDN-193189 (4-[6-(4-piperazin-1-ylphenyl)pyrazolo[1,5-a]pyrimidin-3-yl]quinoline) (LDN), was synthesized, as previously described[19]. ALK3-Fc was provided by Acceleron Pharma Inc. (Cambridge, MA). OsteoSense 680 and ProSense 750 were obtained from PerkinElmer (Waltham, MA). Recombinant human BMP2 and noggin were purchased from R&D Systems (Minneapolis, MN). Human oxLDL was purchased from Intracell Corp. (Frederick, MD). Chloromethyl 2′,7′-dichlorodihydrofluorescein diacetate (CM-H_2DCFDA) was purchased from Invitrogen (Eugene, OR), and lucigenin was purchased from Sigma (St. Louis, MO).

Animals

Eight-week-old female wild-type and $LDLR^{-/-}$ mice on a C57BL/6 background were obtained from Jackson Laboratories (Bar Harbor, ME). Animals were fed a western-style diet formulated to match Paigen's Atherogenic Rodent Diet (42% fat, 0.15% cholesterol, and 19.5% casein; Research Diets Inc., New Brunswick, NJ).

Near-infrared imaging and quantitation of vascular calcific and atherosclerotic lesions

Animals were injected with OsteoSense 680 and ProSense 750 (150 μl each) via the tail vein 24 hours before euthanasia, as described previously[21, 22]. OsteoSense 680 (Osteosense) is a bisphosphonate-derivatized near-infrared fluorescent imaging probe which, being incorporated into hydroxyapatite, marks early osteogenic activity in the vasculature and predicts the development of calcified lesions[21]. Prosense 750 (Prosense) is a cathepsin-activated near-infrared imaging agent which has been previously demonstrated to mark the activity of vascular macrophages and reflect atherosclerotic burden[21]. Aortae were dissected and separated from adventitial and myocardial tissue and analyzed *ex vivo* by near-infrared fluorescence reflectance imaging using an Odyssey Imaging System (LI-COR Biotechnology, software version 3.0.16, Lincoln, NE) with signal intensities and volumes determined for regions of interest.

Bone mineral density

Bone mineral density was measured in femurs from sacrificed mice using a dual energy X-ray absorptiometry (DEXA) Scanner from Lunar/GE Medical Systems (PIXImus2, Faxitron X-Ray Corporation, Wheeling, IL) and analyzed using the PIXImus2 software.

Cell Culture

HepG2 cells were purchased from the American Type Culture Collection (Manassas, VA) and maintained in Eagle's Minimum Essential Medium (EMEM) supplemented with 10%

fetal bovine serum, 100 units/ml of penicillin, 0.1 mg/ml of streptomycin and glutamine. For protein secretion and gene expression experiments, HepG2 cells were grown to 70% confluence before incubation in EMEM with 0.1% FBS. Apolipoprotein B100 (ApoB) levels were measured in supernatants from HepG2 cells incubated in EMEM containing 0.5% bovine serum albumin using a human ApoB ELISA kit (Mabtech AB, Nacka Strand, Sweden).

Human aortic endothelial cells (HAECs), EBM-2, and EGM-2 medium were purchased from Lonza, (Basel, Switzerland). During protein secretion and gene expression experiments, HAECs were maintained in EBM-2 with 0.1% FBS without additional growth factors. BMP2 protein levels were measured in supernatants from HAECs incubated in EBM-2 containing 0.1% FBS using a BMP2 ELISA kit (R&D Systems, Minneapolis, MN). For measurements of reactive oxygen species production, HAECs were incubated in serum-free media for six hours prior to the experiment.

Quantitative RT-PCR

Total cellular RNA from cultured cells was extracted by the phenol/guanidine method[23]. Reverse transcription was performed using Moloney murine leukemia virus reverse transcriptase (Promega, Madison, WI, USA). A Mastercycler ep Realplex (Eppendorf, Hamburg, Germany) was used for real-time amplification and quantification of transcripts. Relative expression and changes in the expression of target transcripts were normalized to levels of 18S ribosomal RNA, determined using the relative CT method. Quantitative PCR was performed using primer sequences as provided in Supplementary Table I.

Measurement of reactive oxygen species production

HAECs were plated overnight in a 96-well format. Following starvation in serum-free media for six hours, cells were pre-treated with and without LDN-193189, ALK3-Fc, or noggin for 30 min followed by incubation with vehicle, oxLDL, or BMP2 for 20 hours. H_2O_2 and O_2^- production were measured with CM-H_2DCFDA and lucigenin, respectively, as described previously[24-26].

Histology and immunohistochemistry

For histology, aortae were embedded and cryopreserved in optimal cutting-temperature medium (Sakura Tissue-Tek, Zoeterwoude, Netherlands) before sectioning into 6-μm sections. Paraformaldehyde-fixed aortic tissue samples were used to prepare en face specimens, and stained with Oil Red O to detect lipid. Calcification was detected in cryosections by Alizarin Red or von Kossa staining. To quantify the extent of calcification, equivalent longitudinal sections of the aortic arch including the minor curvature were obtained from mice subjected to various treatments, and the surface areas stained by von Kossa or Alizarin Red were quantified (ImageJ software, NIH, Bethesda, Maryland). To quantify atheroma, whole-mount aortae were subjected to Oil Red O staining and areas of involvement for given regions of interest (root, arhc, carotid bifurcations and thoracic aorta) quantified by a similar approach. For immunofluorescence, frozen tissue sections were post-fixed in cold methanol and incubated with polyclonal antibodies specific for *p*-SMAD1/5/8 (1:100 dilution; Cell Signaling, Danvers, MA) or MAC2 (1:100 dilution; Cedarlane, Burlington, ON) followed by reaction with FITC-labeled goat anti-rabbit IgG (for *p*-SMAD 1/5/8, Jackson Labs, West Grove, PA) or rhodamine-labeled goat anti-rat IgG (for MAC2, Jackson Labs), respectively. Nuclei were identified using using 4′,6-diamidino-2-phenylindole (DAPI). Liver tissues were fixed with paraformaldehyde, embedded in paraffin, and cut in 6μm thick sections. Liver sections were stained with hematoxylin and eosin (H+E).

Serum Analysis

Total cholesterol, triglycerides, and hemoglobin, were analyzed using a HemaTrue™ Hematology Analyzer (Heska AG, Switzerland). Blood urea nitrogen, glucose, alkaline phosphatase, total protein, alanine transaminase, and creatinine were determined using a Spotchem EZ SP-4430 POCT analyzer (Arkray, Inc., Kyoto, Japan). HDL and LDL levels were determined using a fluorescence quantification kit (K613-100, Biovision, Mountain View, CA).

HMG-CoA reductase activity

HMG-CoA reductase activity was measured and quantified using the HMG-CoA Reductase Kit CS1090 (Sigma-Aldrich, St. Louis, MO).

Statistical analysis

Statistical analysis was performed using SPSS 14.0 Data package for Windows (SPSS, Chicago, IL) and Graph Pad Prism 5.02 (GraphPad Software, La Jolla, CA). Data are reported as mean±SEM, unless otherwise indicated. Normal distribution of the data was confirmed using the Shapiro-Wilk-Test. For group comparisons of continuous variables, analysis of variance (ANOVA) with post-hoc Bonferroni-adjusting testing was employed. To determine the relationship between two variables in dose-response experiments, Pearson's rank correlation coefficient was calculated. In all cases, a $p \leq 0.05$ was considered to indicate statistical significance.

Results

Activation and inhibition of the BMP pathway in the vasculature of LDLR$^{-/-}$ mice

Atheroma formation was evident in LDLR$^{-/-}$ mice within 3-6 weeks of beginning a high-fat diet (HFD), followed by development of intimal and medial calcification at 16-20 weeks (Fig. 1a). Also within 3-6 weeks of beginning HFD, phosphorylated BMP-responsive SMADs 1, 5, and 8 (*p*-SMAD1/5/8) were detected in the nuclei of endothelial, intimal macrophages, and medial cells underlying atheromatous lesions (Fig. 1b and Supplementary Fig. I). SMAD1/5/8 activation was most intense at the aortic root and lesser curvature of the aorta. Activation of BMP signaling in vascular lesions persisted for at least 20 weeks (Supplementary Fig. I). To confirm its bioavailability and impact on BMP signaling, LDN-193189 was administered for 5 days (2.5 mg/kg ip daily) to LDLR$^{-/-}$ mice that had received a HFD for 6 weeks. Short-term treatment with LDN-193189 markedly diminished nuclear *p*-SMAD1/5/8 immunoreactivity within atheromatous lesions (Fig. 1c).

Impact of long-term BMP inhibition upon vascular calcification and atherosclerosis

To determine if modifying BMP signaling in the vasculature might prevent the development of vascular calcification in an atherogenic milieu, adult LDLR$^{-/-}$ mice were fed a HFD and simultaneously treated with LDN-193189 (2.5 mg/kg i.p. daily) or vehicle for 20 weeks. Treatment with LDN-193189 appeared to inhibit osteogenic activity in the aortae of LDLR$^{-/-}$ mice, based upon marked reduction of Osteosense labeling (Fig. 2a). A similar reduction in vascular calcification was confirmed by diminished Alizarin red staining (Fig. 2b) or von Kossa silver stain (Supplementary Fig. IIa). The reduction of vascular calcification by treatment with LDN-193189 was accompanied by a marked reduction in vascular inflammation, as determined by Prosense labeling (Fig. 3a). The localization of Osteosense and Prosense labeling were distinct and partially overlapping in merged images (Supplementary Fig. III), as observed previously in other atherosclerotic models[21]. Consistent with an effect of reducing vascular inflammation and atheroma formation, LDN-193189 treatment reduced the aortic Oil Red O staining, which marks lipid-rich

atherosclerotic plaque (Fig. 3b and Supplementary Fig. IIb). Importantly, the impact of LDN-193189 on atherosclerosis and vascular calcification was not associated with a reduction in body weight or food intake (Supplementary Fig. IVa, b). Sustained treatment with LDN-193189 had no significant effect on bone mineral density in $LDLR^{-/-}$ or wild-type animals (Supplementary Fig. V).

To confirm that the effects of LDN-193189 on atherogenesis were mediated by its impact on BMP signaling, a recombinant BMP inhibitor, ALK3-Fc, was administered to HFD-fed $LDLR^{-/-}$ mice for 6 weeks (2 mg/kg i.p. every other day). Treatment with ALK3-Fc markedly reduced vascular *p*-SMAD1/5/8 immunoreactivity and intimal macrophage accumulation (Fig. 4a-b), and significantly reduced cathepsin (Prosense) activity throughout the aorta (Fig. 4c). In certain regions such as the aortic arch and carotid bifurcations, the impact of LDN-193189 upon cathepsin activity was significantly greater than that observed with ALK3-Fc, as administered under this protocol.

Effect of BMP inhibition on endothelial ROS production

A variety of mechanisms have been implicated in the pathogenesis of atherosclerosis. Among these is the induction of ROS synthesis in endothelial cells exposed to oxidized LDL (oxLDL), thought to be a critical event contributing to vascular injury in atherogenesis[27-29]. To gain insight into how BMP inhibition might impact endothelial ROS generation, we measured ROS production in HAECs exposed to oxLDL after pretreatment with vehicle, LDN-193189, ALK3-Fc, or recombinant noggin. Exposure of HAECs to oxLDL increased H_2O_2 and O_2^- production, as reflected by an increase in dichlorofluorescein and lucigenin fluorescence, respectively (Fig. 5a, b). LDN-193189 and ALK3-Fc (Fig. 5b, c), as well as noggin but not control protein (bovine serum albumin, data not shown), attenuated oxLDL-induced ROS production. These results suggested the possibility that oxLDL increases endothelial ROS production via a mechanism requiring BMP ligand expression. In fact, exposure of HAECs to oxLDL for 8 hours increased BMP2 mRNA levels and BMP2 protein expression (Supplementary Fig. VI), similar to observations in other endothelial cell types[30, 31], without significantly altering levels of mRNAs encoding BMP4, BMP6, BMP7, or BMP9 (Fig. 5d). Moreover, incubation of HAECs with BMP2 increased ROS generation in a manner that could also be attenuated by treatment with LDN-193189 or ALK3-Fc (Fig. 5c).

BMP inhibition lowers hepatic cholesterol biosynthesis

Serum lipoprotein levels are known to be an important risk factor for atherosclerosis, and total cholesterol and LDL levels are markedly elevated in HFD-fed $LDLR^{-/-}$ mice (Fig. 6a and Supplementary Table II). We observed that treatment with LDN-193189 reduced total cholesterol levels and LDL levels, but not HDL or triglyceride levels, in $LDLR^{-/-}$ mice fed a HFD for 20 weeks. Similarly, LDN-193189 reduced total serum cholesterol in wild-type animals fed a HFD (Supplementary Table III). The ability of LDN-193189 to reduce LDL levels did not appear to be mediated by a direct effect on HMG CoA reductase (HMGCR) activity (Fig. 6b) or hepatic *HMGCR* gene expression (data not shown).

To further investigate the role of BMP signaling in the regulation of LDL synthesis, we studied production of apolipoprotein B100 (ApoB), the primary LDL apolipoprotein, in a human hepatoma cell line, HepG2. We observed that incubation of HepG2 cells with BMP2 increased ApoB production (Fig. 6c) in a time- and dose-dependent manner (Supplementary Fig. VIIa-b). Incubation with LDN-193189 (Fig. 6c) and ALK3-Fc (Supplementary Fig. VIII) inhibited ApoB production by HepG2 cells in the absence of exogenous BMP2 and prevented the BMP2-induced ApoB secretion. In contrast, the HMGCR inhibitor, atorvastatin, reduced ApoB production in the absence of BMP2 but did not prevent the

induction of ApoB synthesis by BMP2, providing further support for the independence of HMGCR-mediated and BMP-regulated cholesterol biosynthesis.

BMP inhibition with LDN-193189 prevents hepatic steatosis in LDLR$^{-/-}$

Fatty infiltration of the liver or steatosis is known to be an independent risk factor for coronary heart disease and atherosclerosis[32, 33] and is a prominent feature in LDLR$^{-/-}$ mice receiving a HFD[34, 35]. Recent reports have shown that reduction of serum lipoprotein levels can prevent steatosis in LDLR$^{-/-}$ mice[36] and may help to prevent the development of hepatic dysfunction in humans with non-alcoholic steatohepatitis[37, 38]. To ascertain the impact of LDN-193189 on steatosis and associated hepatic function, liver histology and biochemical liver function tests were performed in these animals. LDLR$^{-/-}$ mice fed a HFD for 20 weeks and treated with vehicle exhibited severe steatosis in hepatic tissues, which was markedly reduced in LDN-193189-treated animals (Fig. 6d). Consistent with the reduction in steatosis, treatment with LDN-193189 reduced blood alanine transaminase (ALT) and alkaline phosphatase (ALP) levels in LDLR$^{-/-}$ mice (Supplementary Tables II and IV).

Discussion

We report that pharmacologic inhibition of BMP signaling reduced vascular calcification in atherogenic animals, likely by limiting antecedent atherogenesis and vascular inflammation. We confirm in LDLR$^{-/-}$ mice, as has been recently shown in ApoE$^{-/-}$ mice, that early atherosclerotic lesions are marked by the activation of the BMP signaling pathway in the vascular endothelium, smooth muscle, and subintimal macrophages[16, 39]. A small molecule BMP inhibitor attenuated the activation of SMAD1/5/8 and subsequent vascular inflammation and atheroma—results which were replicated using a complementary BMP ligand trap strategy. These pharmacologic approaches overcome some of the limitations of genetic over-expression and targeted-disruption strategies to implicate BMP signaling definitively in atherogenesis and associated vascular calcification. Moreover, some of the evidence implicating BMP signaling in the pathogenesis of vascular calcification has been based upon the impact of disrupting MGP, and the notion that MGP functions primarily as a BMP inhibitor. However, some recent data suggest that MGP may inhibit vascular calcification via mechanisms that are independent of its ability to inhibit BMP signaling, such as the direct inhibition of hydroxyapatite formation[40]. While the overexpression and deficiency of MGP in mice on an ApoE$^{-/-}$ background result in decreased and increased vascular calcification, respectively, both strains exhibit decreased atherosclerosis, suggesting that the mechanisms by which MGP modulates vascular calcification and atherosclerosis may be distinct[16]. In contrast to previous models, the present data suggest that atherosclerosis and associated vascular calcification are closely coupled and are both enhanced by BMP signaling in the vasculature.

BMP signaling was found to be required for the induction of ROS in endothelial cells by oxLDL, a critical process in atherogenesis[25, 41, 42]. BMP signaling and ROS both enhance the osteogenic differentiation of smooth muscle cells and may, thereby, contribute to subsequent vascular calcification[43-45]. BMP ligands have been previously reported to enhance ROS production in endothelial cells via the activation of NADPH oxidase 1, resulting in the induction of monocyte adhesion factor ICAM-1, COX-2, and a pro-inflammatory transcriptional program[25, 46, 47]. Thus, our observation that oxLDL stimulates HAECs to generate ROS in a BMP-dependent manner is consistent with the notion that BMP signaling mediates vascular inflammation via pro-inflammatory effects of lipid-mediated endothelial injury, and provides a potential explanation of the marked decrease in macrophage recruitment observed in LDN-193189-treated animals. Given recent evidence that BMP signaling may modulate macrophage function and cytokine expression[48-49], a

direct impact of BMP inhibition on macrophages cannot be excluded and would be an important subject of future investigation.

The observation that inhibition of the BMP type I receptor activity with LDN-193189 reduced lipoprotein levels and hepatic steatosis in $LDLR^{-/-}$ mice, as well as BMP2-induced lipoprotein synthesis *in vitro*, suggested the possibility that inhibition of BMP signaling reduced atherogenesis exclusively by reducing LDL levels. However, treatment of hyperlipidemic mice with ALK3-Fc nearly replicated the effects of LDN-193189 upon atherosclerosis in a short-term (6 week) experiment, and, in contrast to LDN-193189, without impacting cholesterol levels. This latter result supports the notion that BMP inhibition may attenuate atherosclerosis by direct effects on the vasculature, and that the impact of BMP inhibition on atherogenesis does not require a reduction in LDL levels. However, it is possible the increased potency of LDN-193189 in reducing vascular inflammation (Fig. 4c) may be attributable to the reduction of LDL levels seen with LDN-193189 treatment combined with direct vascular effects. There are a number of potential explanations for the differences in the ability of LDN-193189 and Alk3-Fc to reduce LDL levels. We considered the possibility that the reduction in LDL levels seen in mice treated with LDN-193189 was attributable to an “off-target” effect of the small molecule. However, the likelihood of this explanation is reduced by the observation that that LDN-193189, ALK3-Fc, and a third BMP signaling inhibitor, noggin, all reduced ApoB synthesis by HepG2 cells in culture. It is possible that the BMP ligand(s) or receptors responsible for regulating lipoprotein synthesis *in vivo* may be more sensitive to LDN-193189, which acts broadly against the known BMP ligands, versus ALK3-Fc, which targets primarily BMP2 and BMP4[20, 50]. Alternatively, the bioavailability, pharmacokinetics, pharmacodynamics, or potency of ALK3-Fc may make it a less effective inhibitor of hepatic lipoprotein synthesis than LDN-193189, as administered in this study.

The striking impact of LDN-193189 upon hepatic steatosis was likely due to its ability to lower serum cholesterol levels, given the established link between serum cholesterol levels and steatosis[34]. With a prevalence of 20-30% in Western adults and 70-90% among obese or diabetic patients, non-alcoholic fatty liver disease (NAFLD) constitutes a novel landmark feature of the metabolic syndrome[51]. Since NAFLD appears to be an independent risk factor for cardiovascular disease[51], therapeutic interventions for asymptomatic NAFLD may yield benefits beyond protecting hepatic function. Whether the reduction in steatosis seen in our model was mediated by effects on lipid metabolism or other hepatic effects of LDN-193189 remains to be determined.

Given the pleiotropic roles of BMP signaling in regulating cell growth and differentiation, necessary caution about pharmacologic BMP inhibition is warranted. While previous studies have examined the effects of LDN-193189 at similar doses in neonatal and adult mice for up to 60 days[20, 50], the current study extends these findings to mice treated for 140 days in $LDLR^{-/-}$ and 210 days in WT animals. Surprisingly, treatment with LDN-193189 did not have significant effects on bone mineral density, nor did it elicit evidence of renal, hepatic, or hematopoietic toxicity, despite having measurable effects on tissue SMAD1/5/8 activation and serum alkaline phosphatase as administered. The limited impact of LDN-193189 upon postnatal skeletogenesis might potentially be explained by studies by Tsuji et al. demonstrating that prototypic BMP ligands BMP2 and BMP4 are dispensable for skeletogenesis when ablated from the limb bud during embryogenesis[52, 53], indicating that signals other than BMP may predominate in this process. These investigators also found that BMP4 was dispensable for fracture healing, whereas BMP2 was necessary. These data suggest that prolonged suppression of BMP signaling in adult animals may be well-tolerated, but more comprehensive toxicology in multiple species and perhaps in fracture

healing models would be necessary to confirm the safety of BMP inhibition as a long-term therapy.

This investigation highlights the BMP signaling pathway as a therapeutic target in the treatment of vascular calcification and atherosclerosis, confirming the role of BMP signaling in regulating vascular oxidative stress and inflammation, while identifying a novel role in lipid metabolism. The HMGCR-independent impact of BMP inhibition on LDL biosynthesis suggests a novel therapeutic strategy for patients who do not tolerate statin medications (i.e., due to statin-induced myopathy, drug sensitivity, chronic hepatic disease, or interactions with other medications) or in whom standard regimens fail to achieve lipid-lowering targets. Given the large unmet need for novel strategies for achieving lipid and cardiovascular risk reduction, the potent effects of BMP signaling modulation upon lipoprotein metabolism is a subject that strongly merits further clinical and mechanistic investigation.

Supplementary Material

Refer to Web version on PubMed Central for supplementary material.

Acknowledgments

The authors wish to thank Drs. R. Peterson, G. Cuny, S. Pearsall, and D. Bloch for experimental advice; Drs. K. Boström, Y. Nagasaka and H. Jo for helpful discussions; and M. Raher for technical assistance.

Source of Funding This work was supported by a research fellowship award of the German Research Foundation (Deutsche Forschungsgemeinschaft, DE-1685-1/1, M.D.), the US National Institutes of Health (T32HL007208, R.M.; AR057374, P.B.Y.), the Leducq Foundation (Multidisciplinary Program to Elucidate the Role of Bone Morphogenetic Protein Signaling in the Pathogenesis of Pulmonary and Systemic Vascular Diseases, K.D.B. and P.B.Y.), the Massachusetts Technology Transfer Center, Boston MA, USA (P.B.Y.), and the Howard Hughes Medical Institute (P.B.Y.).

References

1. Chen D, Zhao M, Mundy GR. Bone morphogenetic proteins. Growth Factors. 2004; 22:233–241. [PubMed: 15621726]
2. Massague J. How cells read TGF-beta signals. Nat Rev Mol Cell Biol. 2000; 1:169–178. [PubMed: 11252892]
3. Miyazono K, Maeda S, Imamura T. BMP receptor signaling: Transcriptional targets, regulation of signals, and signaling cross-talk. Cytokine Growth Factor Rev. 2005; 16:251–263. [PubMed: 15871923]
4. Xia Y, Yu PB, Sidis Y, Beppu H, Bloch KD, Schneyer AL, Lin HY. Repulsive guidance molecule RGMa alters utilization of bone morphogenetic protein (BMP) type II receptors by BMP2 and BMP4. J Biol Chem. 2007; 282:18129–18140. [PubMed: 17472960]
5. Barbara NP, Wrana JL, Letarte M. Endoglin is an accessory protein that interacts with the signaling receptor complex of multiple members of the transforming growth factor-beta superfamily. J Biol Chem. 1999; 274:584–594. [PubMed: 9872992]
6. Boström K, Watson KE, Horn S, Wortham C, Herman IM, Demer LL. Bone morphogenetic protein expression in human atherosclerotic lesions. J. Clin. Invest. 1993; 91:1800–1809. [PubMed: 8473518]
7. Neven E, Dauwe S, De Broe ME, D'Haese PC, Persy V. Endochondral bone formation is involved in media calcification in rats and in men. Kidney Int. 2007; 72:574–581. [PubMed: 17538568]
8. Dhore CR, Cleutjens JP, Lutgens E, Cleutjens KB, Geusens PP, Kitslaar PJ, Tordoir JH, Spronk HM, Vermeer C, Daemen MJ. Differential expression of bone matrix regulatory proteins in human atherosclerotic plaques. Arterioscler. Thromb. Vasc. Biol. 2001; 21:1998–2003. [PubMed: 11742876]

9. Sage AP, Tintut Y, Demer LL. Regulatory mechanisms in vascular calcification. Nat. Rev. Cardiol. 2010; 7:528–536. [PubMed: 20664518]
10. Boström K, Demer LL. Regulatory mechanisms in vascular calcification. Crit. Rev. Eukaryot Gene. Expr. 2000; 10:151–158. [PubMed: 11186330]
11. Boström KI, Jumabay M, Matveyenko A, Nicholas SB, Yao Y. Activation of vascular bone morphogenetic protein signaling in diabetes mellitus. Circ Res. 2011; 108:446–457. [PubMed: 21193740]
12. Nakagawa Y, Ikeda K, Akakabe Y, Koide M, Uraoka M, Yutaka KT, Kurimoto-Nakano R, Takahashi T, Matoba S, Yamada H, Okigaki M, Matsubara H. Paracrine osteogenic signals via bone morphogenetic protein-2 accelerate the atherosclerotic intimal calcification in vivo. Arterioscler. Thromb. Vasc. Biol. 2010; 30:1908–1915. [PubMed: 20651281]
13. Murshed M, Schinke T, McKee MD, Karsenty G. Extracellular matrix mineralization is regulated locally; different roles of two gla-containing proteins. J. Cell. Biol. 2004; 165:625–630. [PubMed: 15184399]
14. Boström K, Tsao D, Shen S, Wang Y, Demer LL. Matrix GLA protein modulates differentiation induced by bone morphogenetic protein-2 in C3H10T1/2 cells. J Biol Chem. 2001; 276:14044–14052. [PubMed: 11278388]
15. Zebboudj AF, Imura M, Boström K. Matrix GLA protein, a regulatory protein for bone morphogenetic protein-2. J Biol Chem. 2002; 277:4388–4394. [PubMed: 11741887]
16. Yao Y, Bennett BJ, Wang X, Rosenfeld ME, Giachelli C, Lusis AJ, Boström KI. Inhibition of Bone Morphogenetic Proteins Protects Against Atherosclerosis and Vascular Calcification. Circ. Res. 2010; 107:485–494. [PubMed: 20576934]
17. Hsu JJ, Tintut Y, Demer LL. Murine models of atherosclerotic calcification. Curr. Drug Targets. 2008; 9:224–228. [PubMed: 18336241]
18. Ishibashi S, Goldstein JL, Brown MS, Herz J, Burns DK. Massive xanthomatosis and atherosclerosis in cholesterol-fed low density lipoprotein receptor-negative mice. J. Clin. Invest. 1994; 93:1885–1893. [PubMed: 8182121]
19. Cuny GD, Yu PB, Laha JK, Xing X, Liu JF, Lai CS, Deng DY, Sachidanandan C, Bloch KD, Peterson RT. Structure-activity relationship study of bone morphogenetic protein (BMP) signaling inhibitors. Bioorg. Med. Chem. Lett. 2008; 18:4388–4392. [PubMed: 18621530]
20. Steinbicker AU, Sachidanandan C, Vonner AJ, Yusuf RZ, Deng DY, Lai CS, Rauwerdink KM, Winn JC, Saez B, Cook CM, Szekely BA, Roy CN, Seehra JS, Cuny GD, Scadden DT, Peterson RT, Bloch KD, Yu PB. Inhibition of bone morphogenetic protein signaling attenuates anemia associated with inflammation. Blood. 2011; 117:4915–4923. [PubMed: 21393479]
21. Aikawa E, Nahrendorf M, Figueiredo JL, Swirski FK, Shtatland T, Kohler RH, Jaffer FA, Aikawa M, Weissleder R. Osteogenesis associates with inflammation in early-stage atherosclerosis evaluated by molecular imaging in vivo. Circulation. 2007; 116:2841–2850. [PubMed: 18040026]
22. Aikawa E, Nahrendorf M, Sosnovik D, Lok VM, Jaffer FA, Aikawa M, Weissleder R. Multimodality molecular imaging identifies proteolytic and osteogenic activities in early aortic valve disease. Circulation. 2007; 115:377–386. [PubMed: 17224478]
23. Chomczynski P, Sacchi N. Single-step method of RNA isolation by acid guanidinium thiocyanate-phenol-chloroform extraction. Anal. Biochem. 1987; 162:156–159. [PubMed: 2440339]
24. Ichinose F, Buys ES, Neilan TG, Furutani EM, Morgan JG, Jassal DS, Graveline AR, Searles RJ, Lim CC, Kaneki M, Picard MH, Scherrer-Crosbie M, Janssens S, Liao R, Bloch KD. Cardiomyocyte-specific overexpression of nitric oxide synthase 3 prevents myocardial dysfunction in murine models of septic shock. Circ. Res. 2007; 100:130–139. [PubMed: 17138944]
25. Sorescu GP, Song H, Tressel SL, Hwang J, Dikalov S, Smith DA, Boyd NL, Platt MO, Lassegue B, Griendling KK, Jo H. Bone morphogenic protein 4 produced in endothelial cells by oscillatory shear stress induces monocyte adhesion by stimulating reactive oxygen species production from a nox1-based NADPH oxidase. Circ. Res. 2004; 95:773–779. [PubMed: 15388638]
26. Abid MR, Spokes KC, Shih SC, Aird WC. NADPH oxidase activity selectively modulates vascular endothelial growth factor signaling pathways. J. Biol. Chem. 2007; 282:35373–35385. [PubMed: 17908694]

27. Levitan I, Volkov S, Subbaiah PV. Oxidized LDL: diversity, patterns of recognition, and pathophysiology. Antioxid. Redox Signal. 2010; 13(1):39–75. [PubMed: 19888833]
28. Mody N, Parhami F, Sarafian TA, Demer LL. Oxidative stress modulates osteoblastic differentiation of vascular and bone cells. Free Radic. Biol. Med. 2001; 31:509–519. [PubMed: 11498284]
29. Shao JS, Aly ZA, Lai CF, Cheng SL, Cai J, Huang E, Behrmann A, Towler DA. Vascular Bmp Msx2 Wnt signaling and oxidative stress in arterial calcification. Ann. N. Y. Acad. Sci. 2007; 1117:40–50. [PubMed: 18056036]
30. Su X, Ao L, Shi Y, Johnson TR, Fullerton DA, Meng X. Oxidized Low Density Lipoprotein Induces Bone Morphogenetic Protein-2 in Coronary Artery Endothelial Cells via Toll-like Receptors 2 and 4. J. Biol. Chem. 2011; 286:12213–12220. [PubMed: 21325271]
31. Zhang M, Zhou SH, Li XP, Shen XQ, Fang ZF, Liu QM, Qiu SF, Zhao SP. Atorvastatin downregulates BMP-2 expression induced by oxidized low-density lipoprotein in human umbilical vein endothelial cells. Circ J. 2008; 72:807–812. [PubMed: 18441463]
32. Gastaldelli A, Kozakova M, Hojlund K, Flyvbjerg A, Favuzzi A, Mitrakou A, Balkau B. Fatty liver is associated with insulin resistance, risk of coronary heart disease, and early atherosclerosis in a large European population. Hepatology. 2009; 49:1537–1544. [PubMed: 19291789]
33. Fabbrini E, Magkos F, Mohammed BS, Pietka T, Abumrad NA, Patterson BW, Okunade A, Klein S. Intrahepatic fat, not visceral fat, is linked with metabolic complications of obesity. Proc Natl Acad Sci U S A. 2009; 106:15430–15435. [PubMed: 19706383]
34. Rodriguez-Sanabria F, Rull A, Aragones G, Beltran-Debon R, Alonso-Villaverde C, Camps J, Joven J. Differential response of two models of genetically modified mice fed with high fat and cholesterol diets: relationship to the study of non-alcoholic steatohepatitis. Mol Cell Biochem. 2010; 343:59–66. [PubMed: 20512524]
35. Hartvigsen K, Binder CJ, Hansen LF, Rafia A, Juliano J, Horkko S, Steinberg D, Palinski W, Witztum JL, Li AC. A diet-induced hypercholesterolemic murine model to study atherogenesis without obesity and metabolic syndrome. Arterioscler. Thromb. Vasc. Biol. 2007; 27:878–885. [PubMed: 17255537]
36. Wouters K, van Gorp PJ, Bieghs V, Gijbels MJ, Duimel H, Lutjohann D, Kerksiek A, van Kruchten R, Maeda N, Staels B, van Bilsen M, Shiri-Sverdlov R, Hofker MH. Dietary cholesterol, rather than liver steatosis, leads to hepatic inflammation in hyperlipidemic mouse models of nonalcoholic steatohepatitis. Hepatology. 2008; 48:474–486. [PubMed: 18666236]
37. Athyros VG, Tziomalos K, Daskalopoulos GN, Karagiannis A, Mikhailidis DP. Statin-based treatment for cardiovascular risk and non-alcoholic fatty liver disease. Killing two birds with one stone? Ann Med. 2011; 43:167–171.
38. Maroni L, Guasti L, Castiglioni L, Marino F, Contini S, Macchi V, De Leo A, Gaudio G, Tozzi M, Grandi AM, Cosentino M, Venco A. Lipid Targets During Statin Treatment in Dyslipidemic Patients Affected by Nonalcoholic Fatty Liver Disease. Am J Med Sci. 2011; 342:383–387. [PubMed: 21629037]
39. Yao Y, Shao ES, Jumabay M, Shahbazian A, Ji S, Boström KI. High-density lipoproteins affect endothelial BMP-signaling by modulating expression of the activin-like kinase receptor 1 and 2. Arterioscler Thromb Vasc Biol. 2008; 28:2266–2274. [PubMed: 18948634]
40. Lomashvili KA, Wang X, Wallin R, O'Neill WC. Matrix GLA protein metabolism in vascular smooth muscle and role in uremic vascular calcification. J Biol Chem. 2011; 286:28715–28722. [PubMed: 21705322]
41. Napoli C, Quehenberger O, De Nigris F, Abete P, Glass CK, Palinski W. Mildly oxidized low density lipoprotein activates multiple apoptotic signaling pathways in human coronary cells. FASEB J. 2000; 14:1996–2007. [PubMed: 11023984]
42. Hulsmans M, Holvoet P. The vicious circle between oxidative stress and inflammation in atherosclerosis. J. Cell. Mol. Med. 2010; 14:70–78. [PubMed: 19968738]
43. Muteliefu G, Enomoto A, Jiang P, Takahashi M, Niwa T. Indoxyl sulphate induces oxidative stress and the expression of osteoblast-specific proteins in vascular smooth muscle cells. Nephrol Dial Transplant. 2009; 24:2051–2058. [PubMed: 19164326]

44. Speer MY, Yang HY, Brabb T, Leaf E, Look A, Lin WL, Frutkin A, Dichek D, Giachelli CM. Smooth muscle cells give rise to osteochondrogenic precursors and chondrocytes in calcifying arteries. Circ Res. 2009; 104:733–741. [PubMed: 19197075]
45. Yu PB, Deng DY, Beppu H, Hong CC, Lai C, Hoyng SA, Kawai N, Bloch KD. Bone morphogenetic protein (BMP) type II receptor is required for BMP-mediated growth arrest and differentiation in pulmonary artery smooth muscle cells. J Biol Chem. 2008; 283:3877–3888. [PubMed: 18042551]
46. Sorescu GP, Sykes M, Weiss D, Platt MO, Saha A, Hwang J, Boyd N, Boo YC, Vega JD, Taylor WR, Jo H. Bone morphogenic protein 4 produced in endothelial cells by oscillatory shear stress stimulates an inflammatory response. J Biol Chem. 2003; 278:31128–31135. [PubMed: 12766166]
47. Wong WT, Tian XY, Chen Y, Leung FP, Liu L, Lee HK, Ng CF, Xu A, Yao X, Vanhoutte PM, Tipoe GL, Huang Y. Bone Morphogenic Protein-4 Impairs Endothelial Function Through Oxidative Stress-Dependent Cyclooxygenase-2 Upregulation. Implications on Hypertension. Circ Res. 2010; 107:984–91.
48. Wang L, Harrington L, Trebicka E, Shi HN, Kagan JC, Hong CC, Lin HY, Babitt JL, Cherayil BJ. Selective modulation of TLR4-activated inflammatory responses by altered iron homeostasis in mice. J Clin Invest. 2009; 119:3322–3328. [PubMed: 19809161]
49. Lee GT, Kwon SJ, Lee JH, Jeon SS, Jang KT, Choi HY, Lee HM, Kim WJ, Kim SJ, Kim IY. Induction of interleukin-6 expression by bone morphogenetic protein-6 in macrophages requires both SMAD and p38 signaling pathways. J Biol Chem. 2010; 285:39401–39408. [PubMed: 20889504]
50. Yu PB, Deng DY, Lai CS, Hong CC, Cuny GD, Bouxsein ML, Hong DW, McManus PM, Katagiri T, Sachidanandan C, Kamiya N, Fukuda T, Mishina Y, Peterson RT, Bloch KD. BMP type I receptor inhibition reduces heterotopic ossification. Nat Med. 2008; 14:1363–1369. [PubMed: 19029982]
51. Targher G, Bertolini L, Padovani R, Rodella S, Zoppini G, Pichiri I, Sorgato C, Zenari L, Bonora E. Prevalence of non-alcoholic fatty liver disease and its association with cardiovascular disease in patients with type 1 diabetes. J Hepatol. 53:713–718. [PubMed: 20619918]
52. Tsuji K, Cox K, Bandyopadhyay A, Harfe BD, Tabin CJ, Rosen V. BMP4 is dispensable for skeletogenesis and fracture-healing in the limb. J Bone Joint Surg Am. 2008; 90(Suppl 1):14–18. [PubMed: 18292351]
53. Tsuji K, Bandyopadhyay A, Harfe BD, Cox K, Kakar S, Gerstenfeld L, Einhorn T, Tabin CJ, Rosen V. BMP2 activity, although dispensable for bone formation, is required for the initiation of fracture healing. Nat Genet. 2006; 38:1424–1429. [PubMed: 17099713]

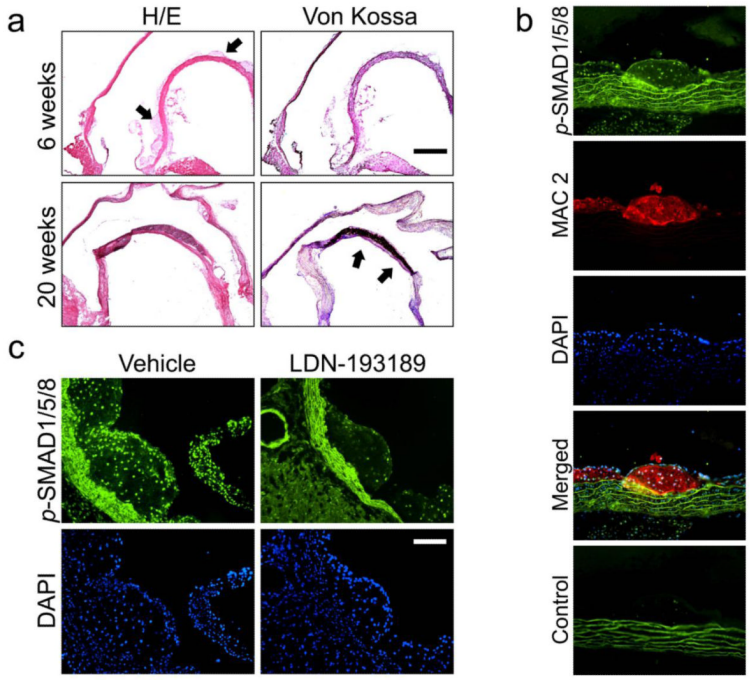

Figure 1. The BMP signaling pathway is activated within atherosclerotic lesions in LDLR$^{-/-}$ mice on a high fat diet

(a) Serial coronal sections of aortae from two representative LDLR$^{-/-}$ from mice fed HFD for either 6 (n=20) or 20 weeks (n=20) were stained with hematoxylin and eosin (H+E, left) or with von Kossa (right). After 6 weeks on HFD, atherosclerotic lesions without calcification appeared (top left panel; arrows indicate atheromatous lesions in the aortic root and minor curvature). Severe medial calcification was detectable after 20 weeks on HFD (von Kossa, lower right panel; arrows indicate medial calcification in the aortic minor curvature). Bar indicates 500 μm. **(b)** Immunofluorescence of sections from the minor curvature of the aorta from an LDLR$^{-/-}$ mouse fed HFD for 6 weeks (n=20) revealed activated SMAD1/5/8 (*p*-SMAD1/5/8, green), intimal macrophages (MAC2, red), with nuclear counterstain (DAPI, blue). Atheromatous lesions consisted predominantly of macrophages bordered by endothelium and media, all of which revealed intense nuclear staining for *p*-SMAD1/5/8. (White bar=100 μm). **(c)** LDLR$^{-/-}$ mice were fed a HFD for six weeks and treated with vehicle or LDN-193189 (n=4, 2.5 mg/kg ip daily) for the last five days before harvesting. Immunofluorescence of aortic sections obtained from vehicle-treated animals (n=4, left panels) revealed abundant nuclear *p*-SMAD1/5/8 within atheromatous lesions in the aortic root (green, upper panels; blue DAPI counterstain, lower panels), which was markedly suppressed in LDN-193189-treated animals. (White bar=100 μm)

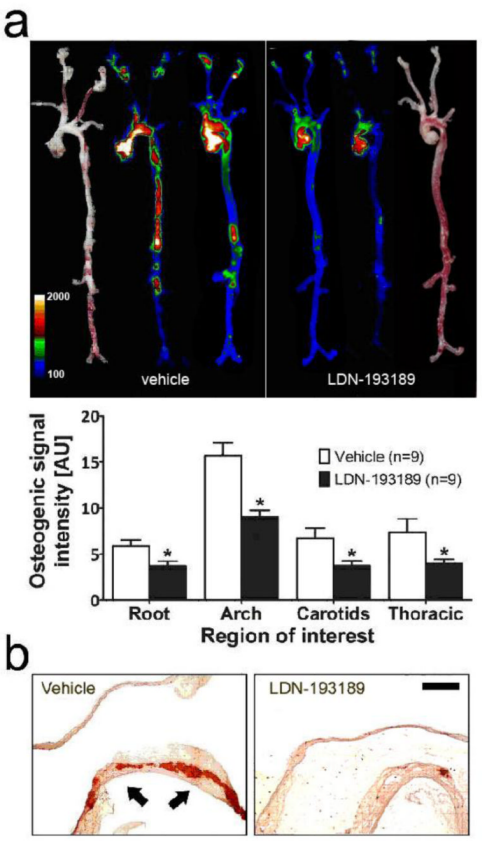

Figure 2. Treatment with a BMP antagonist prevents arterial calcification in LDLR$^{-/-}$

Aortae were harvested from HFD-fed LDLR$^{-/-}$ mice treated with vehicle (n=20, left) or LDN-193189 (n=20, 2.5 mg/kg ip daily, right) for 20 weeks. **(a)** Aortae were dissected and imaged by near-infrared fluorescence reflectance imaging 24h after iv injection with OsteoSense 680 (a near-infrared fluorescent bisphosphonate probe). Brightfield images (outside) provide a reference for intensity maps (inside) obtained from two representative aortae for each treatment group, demonstrating the localization and degree of osteogenic activity. Fluorescence intensities in four regions of interest, the aortic root (Root), aortic arch (Arch), carotid arteries (Carotids), or thoracic aorta (Thoracic), are shown (mean ± SEM, arbitrary units (AU), *p≤0.05 vs. corresponding region of interest in vehicle-treated animals). **(b)** Aortae (representative of 6 mice in each group) were stained with Alizarin red. Abundant Alizarin red staining, representing vascular calcification (indicated with arrows), was evident in the minor curvature of vehicle-treated mice, with markedly diminished Alizarin red staining in aortae from LDN-193189-treated mice. Bar indicates 500 μm.

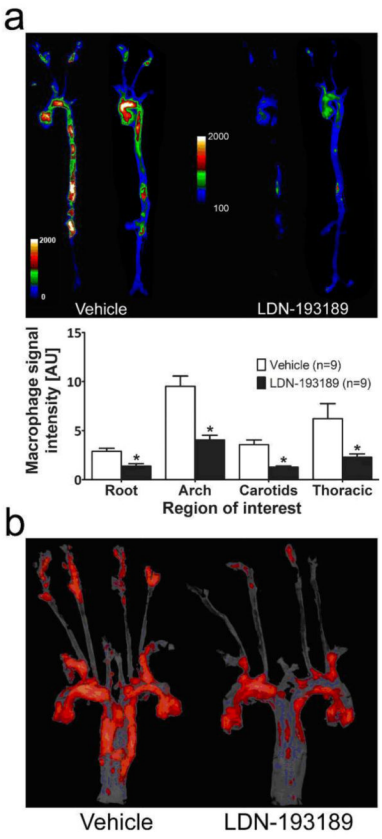

Figure 3. Treatment with a BMP antagonist prevents atherosclerosis in LDLR$^{-/-}$

Aortae were harvested from HFD-fed LDLR$^{-/-}$ mice treated with vehicle (n=20, left) or LDN-193189 (n=20, 2.5 mg/kg ip daily, right) for 20 weeks. **(a)** Near-infrared fluorescence images demonstrating localization and intensity of macrophage activity as determined using Prosense 750, a fluor-labeled cathepsin substrate. Intensity maps obtained from two representative aortae for each treatment group demonstrate localization and degree of macrophage activity. Fluorescence intensities in four regions of interest, the aortic root (Root), aortic arch (Arch), carotid arteries (Carotids), or thoracic aorta (Thoracic), are shown (mean ± SEM, arbitrary units (AU), *p≤0.05 vs. corresponding region of interest in vehicle-treated animals). **(b)** En face staining with Oil Red O demonstrated diminished lipid plaque in the aortae of LDN-193189-treated animals, representing results from 6 vehicle- and 6 drug-treated mice.

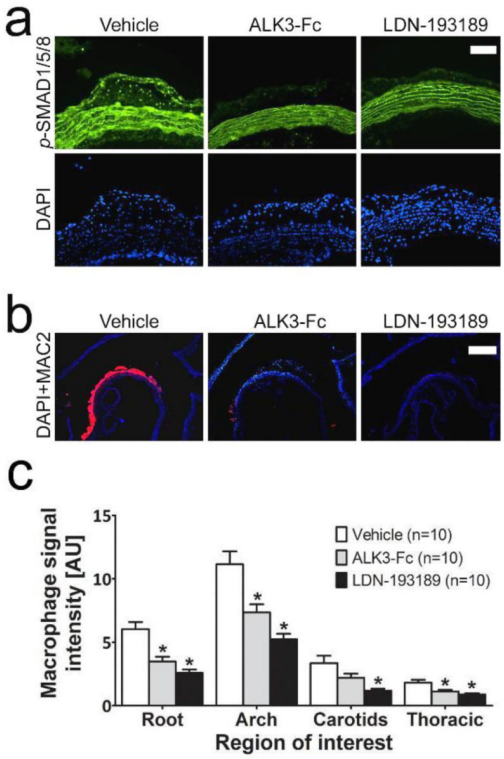

Figure 4. LDN-193189 effects on atherosclerosis are BMP mediated

Tissues in panels (a)-(c) were harvested from LDLR$^{-/-}$ mice on HFD for 6 weeks, which were treated with vehicle (left side), ALK3-Fc (2 mg/kg ip, every other day, middle) or LDN-193189 (2.5 mg/kg ip daily, right side) for five days (n=4 in each group, **a**) or 6 weeks (n=10 in each group, **b+c**) prior to harvesting. **(a)** Immunofluorescence of aortic sections revealed nuclear *p*-SMAD1/5/8 (green, DAPI counterstain, blue) in atheromatous lesions, which was markedly suppressed by either LDN-193189 or ALK3-Fc treatment (white bar=100 μm). **(b)** Immunofluorescence of aortic sections revealed the accumulation of intimal macrophages (MAC2, red; DAPI counterstain, blue), which was markedly diminished by LDN-193189 or ALK3-Fc (White bar=500 μm). **(c)** Near-infrared fluorescence intensities of Prosense 750 revealed suppression of macrophage activity by ALK3-Fc and LDN-193189 treatment in nearly all regions of interest.

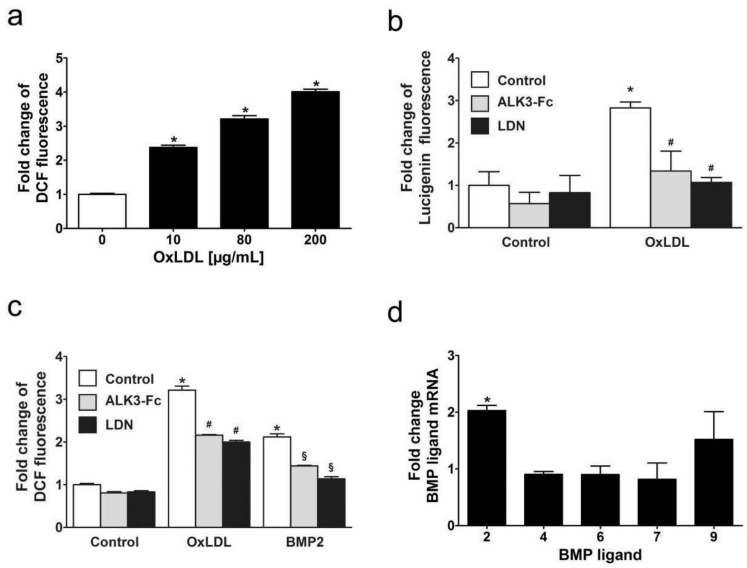

Figure 5. ROS production is induced by oxLDL in HAECs in a BMP-dependent manner

(a) Oxidized LDL induced the production of hydrogen peroxide in a dose-dependent manner in human aortic endothelial cells. HAECs were incubated with the indicated concentrations of oxLDL for 20 hours in EGM-2 media containing 0.1% fetal bovine serum. Fluorescence intensities were measured at 527 nm after incubating the cells for 60 minutes with chloromethyl 2′,7′-dichlorodihydrofluorescein diacetate (DCF). Data presented as mean ±SEM. *p≤0.05 versus cells not exposed to oxLDL (n=6 measurements for each condition).

(b) Oxidized LDL cholesterol induced generation of reactive oxygen species in human aortic endothelial cells, as estimated with lucigenin fluorescence. HAECs were incubated without (Control) or with oxLDL (80 μg/mL) for 20 hours in EGM-2 media containing 0.1% fetal bovine serum. Induction of ROS by oxLDL was markedly reduced by pretreatment with LDN-193189 (LDN, 100 nM) or ALK3-Fc (500 ng/mL). Data presented as mean ±SEM. *p≤0.05 vs. Control. $^{\#}$p≤0.05 vs. treatment with oxLDL alone (n=6 measurements for each condition).

(c) Incubation of HAECs with oxLDL (80 μg/mL) or BMP2 (20 ng/mL) induced hydrogen peroxide production, as quantified by measuring DCF fluorescence. Induction of hydrogen peroxide production by both oxLDL and BMP2 was inhibited by pretreatment with LDN-193189 (LDN, 100 nM) or ALK3-Fc (500 ng/mL). Differences among controls were significant (p=0.01 comparing LDN to control, p=0.009 comparing ALK3-Fc versus control). (n=6 measurements for each condition, *p≤0.05 vs. control without treatment, $^{\#}$p≤0.05 vs. treatment with oxLDL alone, §p≤0.05 vs. treatment with BMP2 alone).

(d) BMP2 mRNA levels were induced in human aortic endothelial cells by oxLDL. HAECs were incubated with oxLDL (80 μg/mL) for eight hours, and levels of mRNAs encoding BMP ligands were measured by qRT-PCR. (n=4 measurements for each condition, *p≤0.05 vs. control without treatment).

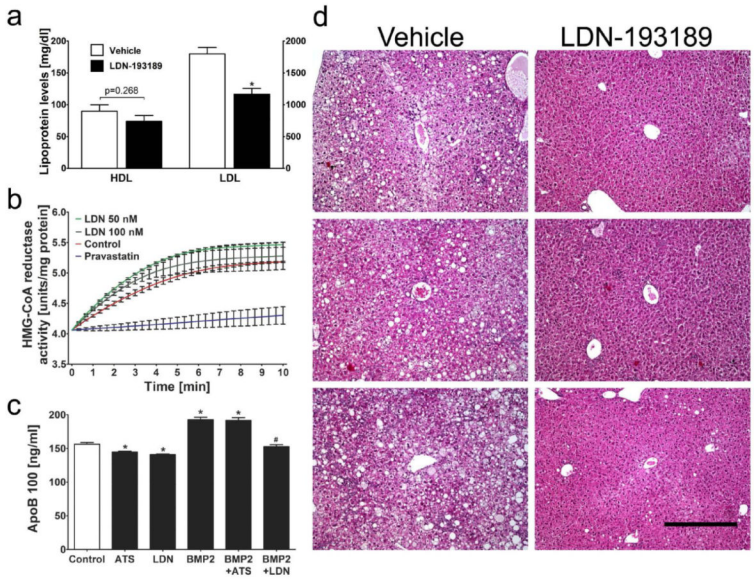

Figure 6. BMP inhibition lowers hepatic cholesterol biosynthesis

(a) Serum HDL and LDL levels were measured in HFD-fed LDLR$^{-/-}$ mice treated with vehicle (n=8) or LDN-193189 (n=7, 2.5 mg/kg ip, daily) for 20 weeks. Serum LDL cholesterol levels were reduced by 35% in LDN-193189-treated mice as compared to vehicle-treated mice(1166±241 vs. 1797±289 mg/dl), while HDL cholesterol levels were not altered (74±25 vs. 90±28 mg/dl). (*p≤0.05 vs. vehicle treatment; HDL values plotted on left, LDL plotted on right y-axis)

(b) LDN-193189 did not inhibit HMG-CoA reductase in vitro. HMG-CoA reductase enzyme activity was measured in vitro in the absence (Control) or presence of LDN-193189 (LDN, 50 nM and 100 nM) or pravastatin. Pravastatin, but not LDN-193189, inhibited HMG-CoA reductase activity. Data presented as mean±SEM, n=3 measurements.

(c) HepG2 cells were incubated for 24h with or without BMP2 (100 ng/mL) in the presence or absence of an HMG-CoA reductase inhibitor, atorvastatin (ATS, 1 μM), or LDN-193189 (LDN, 100 nM). Apolipoprotein B100 (ApoB 100) levels in the culture medium were measured. *p≤0.05 vs. untreated HepG2 cells (Control), $^{\#}$p≤0.05 vs. HepG2 cells incubated with BMP2, n=4 measurements.

(d) Hepatic tissue sections from HFD-fed LDLR$^{-/-}$ mice treated with either vehicle (n=20, left) or LDN-193189 (n=20, 2.5 mg/kg ip, daily; right) for 20 weeks were stained with H+E and photographed. Liver sections from three mice (representative of six) from each group are shown. LDN-193189 protects HFD-fed mice from hepatic steatosis. (Bar=400 μm).